PHYSICAL REVIEW A **69**, 051402(R) (2004)

Measurement of hydrogenic tunneling rates in a high-intensity laser focus

B. Buerke*,† and D. D. Meyerhofer*,‡
Laboratory for Laser Energetics, University of Rochester, 250 East River Road, Rochester, New York 14623-1299, USA
(Received 7 January 2004; published 7 May 2004)

An accurate measurement of the tunneling ionization rate for the hydrogenic ground state of helium (He^{1+}) in a circularly polarized, 2-ps, high-intensity laser pulse is presented. The ionizing electric fields are determined with an uncertainty of less than 2% by measuring the energies of electrons ponderomotively accelerated out of the focus. The inferred ionization rate agrees well with semiclassical and exact solutions of the Schrödinger equation.

DOI: 10.1103/PhysRevA.69.051402 PACS number(s): 32.80.Rm, 32.80.Fb

Tunneling ionization of hydrogenic atoms exposed to a strong electromagnetic field is a classic phenomenon of nonperturbative atomic physics. Tunneling is the static strong-field limit of multiphoton ionization, in which the electron escapes from the atom on a time scale (τ_t) much shorter than the field period ($2\pi/\omega$), and is described by the Keldysh parameter [1], $\gamma=\omega\tau_t=\omega(2E_B)^{1/2}/\mathcal{E}$, where $-E_B$ is the binding energy of the atom and $\mathcal{E}$ is the electric field in atomic units. The tunneling regime ($\gamma \ll 2\pi$) is reached either by $\omega \to 0$ or $\mathcal{E} \to \infty$. Under these conditions the atom–field interaction is sufficiently simplified that, for a hydrogenic atom, the Schrödinger equation can be solved exactly [2,3]. The resulting electron behavior is completely characterized by a shift and induced width of the quasibound state, with the latter being proportional to the tunneling rate measured in experiments.

Previous accurate measurements of hydrogenic tunneling rates as a function of field strength, by Koch and Mariani [4], used a weak static electric field ($\sim$500 V/cm) to ionize high Rydberg states of hydrogen (principal quantum number $n=30$, 40) and gave excellent agreement with numerical solutions of the Schrödinger equation. Both microwave [5] and laser [6,7] ionization experiments indicate that atoms exposed to quasi-static fields ionize near the classical threshold [in atomic units (a.u.)]:

$$\mathcal{E}_{\text{classical}} = (E_B)^2/4Z, \tag{1}$$

where Z is the residual charge of the ion. For a hydrogenic ground state, the fields required for ionization ($\mathcal{E} > 10^8$ V/cm) are obtained only in the focus of a high-intensity laser.

Accurate measurements of ground-state tunneling rates as a function of field strength have not been possible to date because ultrahigh laser intensities are notoriously inaccurate, especially when obtained from independent measurements of energy, pulse width, and focal area [6–8]. Intensities are often calibrated by comparing ion-yield data to particular theoretical predictions, but this allows only relative rates to be determined [8–10]. Improved accuracy can be achieved by measuring electron spectra produced by short-pulse resonant multiphoton ionization in conjunction with ion-yield data. Using this approach, Walker *et al.* [10] achieved intensity accuracies of ±25% in studies of nonsequential ionization of helium. Because the tunneling ionization rate varies rapidly with the field strength, even small uncertainties in intensity cause large uncertainties in the value of the ionization rate, in the latter case about a factor of 10.

In this Rapid Communication an accurate measurement of the tunneling ionization rate for the ground state of hydrogenic helium is reported. Due to its large binding energy ($E_B=54.4$ eV$=2$ a.u.), He^{1+} is expected to ionize well into the tunneling regime [$\gamma \sim 0.2-0.3$] for the conditions in this experiment. By measuring the energy of electrons produced by tunneling and ponderomotively accelerated out of the focus, the ionizing fields are determined with a total uncertainty less than 2%. The corresponding ionization rates inferred by comparing theory to the experimental results have an uncertainty less than 30%. The results give excellent agreement with both semiclassical [11] and exact analytic [3] solutions of the Schrödinger equation for a hydrogenic atom ionized by a quasistatic electromagnetic field. The results show that the systematic errors associated with a high-intensity laser focus can be carefully controlled, leading to sensitive tests of tunneling ionization and other nonperturbative effects in strongly driven atoms.

The energy of electrons produced during ionization and ejected from the laser focus is related to the fields at the time of ionization [12]. Under tunneling conditions, electrons acquire both a constant drift energy during the first laser cycle after ionization and a ponderomotive energy while traversing the laser focus. When the laser pulse duration is much longer than the time required for electrons to exit the focus, electrons in a circularly polarized field gain about twice the full quiver energy ($U_p=\mathcal{E}^2/2\omega^2$) available at ionization. For the circularly polarized, 2-ps laser pulse used in this experiment, measuring the final electron energy of $\sim 2U_p$ allows the ionizing field to be determined.

A fully relativistic Monte Carlo simulation [13–16] is used to obtain an accurate calibration between the final elec-

*Also with the Department of Physics and Astronomy, University of Rochester, Rochester, NY 14623, USA.
†Present address: Department of Physics, Albright College, Reading, PA 19604, USA.
‡Also with Department of Mechanical Engineering, University of Rochester, Rochester, NY 14623, USA.

tron energy and the ionizing field. The simulation [13,14] assumes that electrons tunnel instantaneously into the laser field with zero initial velocity [12] and subsequently propagate through a time-dependent Gaussian laser focus via the classical Lorentz force. The assumptions underlying the simulation have been verified experimentally for this laser system [14]. The results of the Monte Carlo simulation will be discussed in detail elsewhere but are summarized here. The final electron energies have a broad Gaussian distribution with an average electron energy close to $2U_p$. However, inelastic ponderomotive scattering on the rising edge of the laser pulse [17] can cause the average electron energy to exceed $2U_p$, reaching a maximum of $\sim 2.2U_p$. By carefully choosing the laser focal parameters to obtain this maximum, the final electron energy becomes highly insensitive to variation in the peak laser intensity (ΔI= factor of $2 \Rightarrow$ energy uncertainty $\sim 0.7\%$). Hence, the fields at ionization are determined accurately not by measuring the peak laser intensity accurately but by eliminating its effect on the final electron energies.

The chirped-pulse-amplification (CPA) laser used in these experiments, producing 2.0-ps pulses at a wavelength of 1.053 μm, has been described elsewhere [18]. After passing through a quarter-wave plate to obtain circular polarization, the laser beam is focused by an aspherical lens ($f=20$ cm, $f/4$) to a Gaussian focal spot of 5 μm ($1/e^2$ radius), giving a peak intensity of 1.5×10^{17} W/cm^2. The vacuum chamber, with a background pressure of 2×10^{-9} Torr, is backfilled with helium to a pressure less than 3×10^{-5} Torr to avoid space-charge effects and detector saturation. The He^{1+} target gas is produced by sequential ionization of neutral helium earlier in the laser pulse [19]. Electrons from both charge states of helium are ejected from the focus, and their energies are measured using a retarding-potential spectrometer, as shown in Fig. 1. Three screens of fine stainless steel mesh (wire diameter =0.0025 cm, 40 wires/cm) are mounted 20 cm from the focus, with the two outer screens grounded and the middle screen connected to a variable negative voltage supply ($-V_R$). The grids are clamped between flat copper rings (hole diameter =2.9 cm) and mounted 2 cm apart, separated by ceramic spacers. Electrons with sufficient energy pass through the screens and are detected by a microchannel plate (MCP). The front of the MCP is biased at +550 V to collect the electrons and make the detection efficiency constant. Triple-layered Co-Netic magnetic shielding [20] surrounds the 28-cm flight path, providing a magnetic field-free ($<$1-mG) region with a detection aperture of 0.0045π sr.

Figure 2 shows the total observed electron signal in picocoulombs versus the electron energy in electron volts (eV_R). Each data point is the average of all the laser shots in a 6% energy bin, adjusted for relative peak intensity and normalized to a pressure of 5×10^{-6} Torr. For the lowest retarding voltages and highest electron signals, the actual pressure is a factor of ten lower to avoid space-charge effects. A single electron hit at the normalized pressure corresponds to $\sim$1 pC. The retarding-potential measurement integrates all the electrons with energies above eV_R, giving, for example, a complementary error-function (erfc) dependence for a Gaussian spectrum. Hence, energy intervals near a peak in

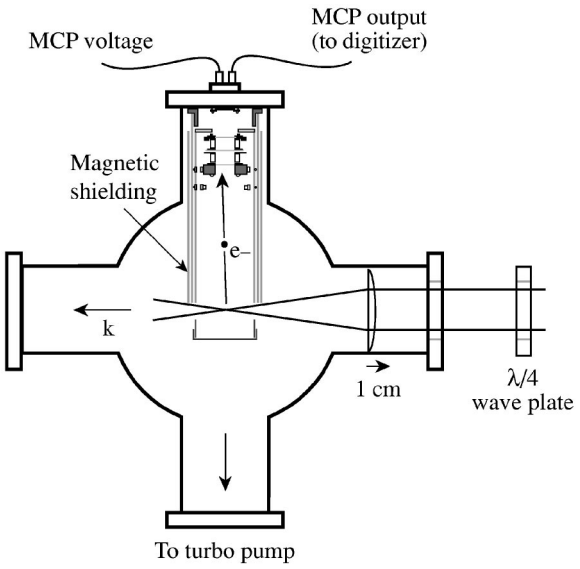

FIG. 1. Vacuum tank setup with retarding-field spectrometer. An electron high-pass filter is created by grounding the two outer grids and negative biasing the center grid. The position of the focus was scanned to test the effects of forward Compton scattering.

the electron energy distribution appear as a large negative slope in the retarding-potential curve. The distribution in Fig. 2 behaves as expected. Electrons from the ionization of neutral helium are evident where the signal falls off from 0 to 700 eV, followed by a flat, electron-free region. Above 1000 eV the signal falls off again, corresponding to electrons from the ionization of He^{1+}.

The solid curve gives the least-squares, double-erfc fit to the data, confirming the Gaussian form of the He^{1+} spectrum. The best-fit values for the Gaussian peak energy and the $1/e$ half-width are 1960 ± 42 eV and 762 ± 51 eV, respectively, where the uncertainties give the 1-σ random error. The energy gained by the electrons is far less than the total energy available at the peak of the pulse at 1.5×10^{17} W/cm^2 ($2U_p=31$ keV). Moreover, the measured spectrum is insen-

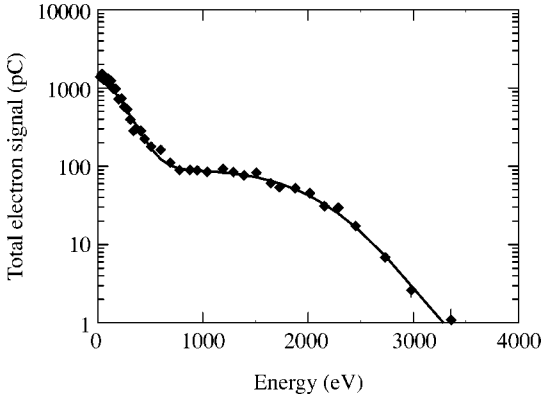

FIG. 2. Retarding-field electron spectrum for the ionization of helium. The vertical axis gives the total measured charge from the MCP in picocoulombs. The horizontal axis is the electron energy (eV_R) calculated from the voltage ($-V_R$) across the retarding grids. The data points are averaged in 6% energy bins. The least-squares fit (solid line) is a double complementary-error function.

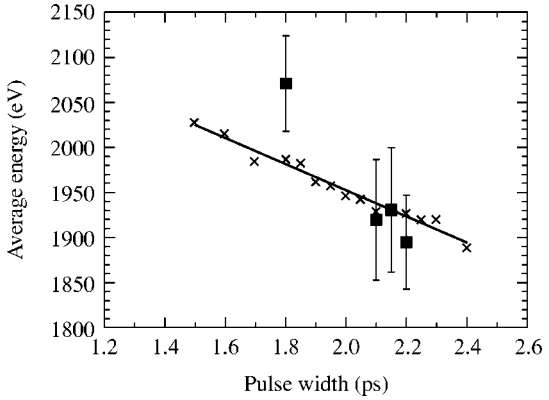

FIG. 3. Average electron energy versus pulse width. Solid squares mark the experimental data points. The solid line is a least-squares linear fit to the simulation results (×'s) for the semiclassical tunneling model.

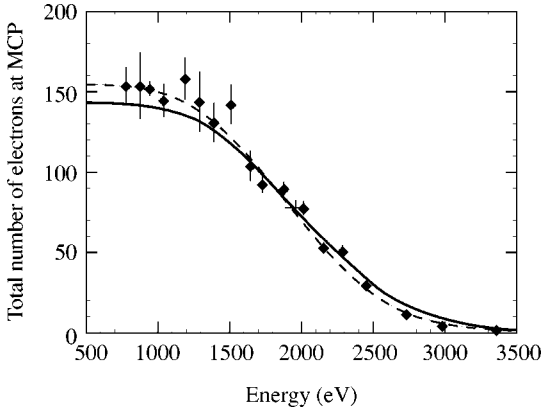

FIG. 4. Retarding-field spectrum for the ionization of He^{1+} compared to the simulation predictions of two tunneling theories. The dashed curve shows the prediction of the semiclassical tunneling model; the solid curve shows the prediction of the exact dc tunneling rate. The horizontal line of the central cross shows the total error for the average energy inferred from the data.

sitive to fluctuations in the peak laser intensity, which differed by a factor of 2 among the various data runs. Consequently, the observed energies represent the intensities at ionization rather than the intensity profile of the focus. The classical threshold for ionization given by Eq. (1) significantly overestimates the field where ionization occurs ($2U_{p,\mathrm{classical}}=3.6$ keV). This is in contrast to experiments with hydrogenic Rydberg states, where Eq. (1) underestimates the observed field [21].

To obtain accurate ionization fields and rates, systematic errors in the experiment were investigated in detail. Potential systematic errors resulting from uncertainties in the pulse width, retarding-voltage measurement, imperfect beam polarization, space charge, nonuniform MCP response versus energy, and a finite detection aperture were experimentally investigated. For example, the finite detection aperture can preferentially cut off high-energy electrons accelerated in the forward direction by multiphoton Compton scattering [13]. This effect was tested by obtaining spectra at various laser focal positions relative to the detection axis (see Fig. 1).

The dominant systematic error comes from uncertainty in the absolute laser pulse width (±15%), which affects both the observed electron energy and the calculated ionization rate. Figure 3 shows the measured average electron energy versus pulse width for four data runs in which full He^{1+} spectra were obtained. The error bars give the statistical uncertainty for each erfc fit. The data are consistent with predictions of Monte Carlo simulations based on the semiclassical ionization rate [11] for He^{1+}, indicated by ×'s. The solid line is the least-squares linear fit to the simulation results. Although the uncertainties in the pulse width data are too large to provide a detailed test of the Monte Carlo predictions, the pulse width scan allows the uncertainty to be reliably determined. Taking into account all likely sources of uncertainty gives a final systematic error of ±3.2% for the average electron energy. The pulse width (±2.3%) and retarding voltage (±2%) are the two main sources of uncertainty, with all other sources contributing less than 0.6%. The systematic error for the energy width (σ) is somewhat larger: +13.6%, −8.2%. For the average energy, adding the random and systematic errors in quadrature gives a total uncertainty of ±3.8%.

The measured energy distribution can be compared to that predicted for the ionization of a hydrogenic ground state in a static electric field. The Schrödinger equation in this case is separable in parabolic coordinates and can be solved analytically. The ground-state ionization rate as a function of the scaled field $\mathcal{E}_s=\mathcal{E}/(2\,E_B)^{3/2}$ is [3]

$$\Gamma(\mathcal{E}_s)=8E_B\frac{1}{\mathcal{E}_s}e^{-2/3E_s}[1-8.92\mathcal{E}_s+25.6(\mathcal{E}_s)^2-159(\mathcal{E}_s)^3+\ldots], \tag{2}$$

where all quantities are in atomic units. The coefficients are known to arbitrarily high order and the expansion is asymptotic. The leading term of this expansion is the semiclassical hydrogenic tunneling rate [11]; the additional terms result from the dc Stark shift of the ground state. For moderate field strengths ($\mathcal{E}_s<1$), the exact rate is less than the semiclassical rate because the downward Stark shift of the ground state binds the electron more tightly and widens the barrier for tunneling.

Figure 4 compares the data for the ionization of He^{1+} with the predictions of both the semiclassical rate (dashed line) and the exact rate given in Eq. (2) (solid line). The cross marks the average energy obtained from the least-squares fit to the experimental data, and the horizontal bar shows the total uncertainty. Both theories agree with the data using *no free parameters*.

The agreement between the observed average energy (1960±75 eV) and the simulation predictions (1929 eV and 2030 eV for semiclassical and exact rates, respectively) is especially important for determining the field strength where ionization is most probable. The simulation indicates that the electrons gain on average 2.203±0.002 times the initial quiver energy, so that $U_p=890\pm34$ eV. This initial quiver energy implies an ionization intensity of $(8.6\pm0.3)\times10^{15}$ W/cm^2 and an ionizing field of $(1.80\pm0.03)\times10^9$ V/cm for hydrogenic helium in a 2.1-ps, 1.053-μm

laser pulse. The corresponding ionization rate is $(3.2^{+1.1}_{-0.8}) \times 10^{12}$ s^{-1}.

The accuracy achieved in this present experiment is limited primarily by the laser's low repetition rate (one shot every 3 min). Using the higher repetition rates currently achievable in CPA systems would allow energy accuracies better than 1%. Experiments with this level of accuracy address important issues in strong-field atomic physics. Tunneling theories based on single-electron dynamics, including the widely used semiclassical theory of Ammosov, Delone, and Krainov (ADK) [22] and the single-active-electron (SAE) approximation [23] have successfully explained experimental observations of the ionization of noble gas atoms and ions [10,24]. In fact, our results confirm that the static-field, semiclassical approach on which ADK is based can be highly accurate in the tunneling regime. In contrast, *ab initio* calculations of tunneling rates in helium [25,26] give higher rates than ADK, which may be due to multielectron effects. The measurements described here are well suited to investigating this issue. In addition, the fully relativistic Monte Carlo simulations can be readily applied to tunneling ionization at relativistic intensities ($I > 10^{18}$ W/cm^2), where accurate tests of tunneling and over-the-barrier theories are desirable [8].

In summary, we have accurately measured the tunneling ionization fields and rates for hydrogenic helium and obtained excellent agreement with semiclassical and exact solutions of the Schrödinger equation. These results show that the systematic errors associated with a high-intensity laser focus can be controlled. This work is important for the study of multielectron atoms in strong fields, and may lead to measurements of dc Stark shifts and relativistic effects.

ACKNOWLEDGMENTS

We gratefully acknowledge C.I. Moore and S.J. McNaught for providing the Monte Carlo simulation codes and J.H. Eberly for fruitful discussions. This work was supported by the National Science Foundation. Additional support was provided the U.S. Department of Energy Office of Inertial Confinement Fusion under Cooperative Agreement No. DE-FC03-92SF19460, the University of Rochester, and the New York State Energy Research and Development Authority. One of us (B.B.) was also supported by Albright College.

[1] L. V. Keldysh, Sov. Phys. JETP **20**, 1307 (1965).
[2] H. J. Silverstone, Phys. Rev. A **18**, 1853 (1978); H. J. Silverstone *et al.*, Phys. Rev. Lett. **43**, 1498 (1979).
[3] H. J. Silverstone, E. Harrell, and C. Grot, Phys. Rev. A **24**, 1925 (1981).
[4] P. M. Koch and D. R. Mariani, Phys. Rev. Lett. **46**, 1275 (1981).
[5] M. G. Littman, M. M. Kash, and D. Kleppner, Phys. Rev. Lett. **41**, 103 (1978).
[6] S. Augst *et al.*, Phys. Rev. Lett. **63**, 2212 (1989).
[7] T. Auguste *et al.*, J. Phys. B **25**, 4181 (1992).
[8] E. Chowdhury, C. P. J. Barty, and B. Walker, Phys. Rev. A **63**, 042712 (2001).
[9] Th. Weber *et al.*, Phys. Rev. Lett. **84**, 443 (2000).
[10] B. Walker *et al.*, Phys. Rev. Lett. **73**, 1227 (1994); **77**, 5031 (1996).
[11] L. D. Landau and E. M. Lifshitz, *Quantum Mechanics—Non-relativistic Theory*, 3rd ed. (Pergamon, New York, 1977), Course of Theoretical Physics, Vol. 3.
[12] P. B. Corkum, N. H. Burnett, and F. Brunel, Phys. Rev. Lett. **62**, 1259 (1989).
[13] C. I. Moore, J. P. Knauer, and D. D. Meyerhofer, Phys. Rev. Lett. **74**, 2439 (1995).
[14] S. J. McNaught, J. P. Knauer, and D. D. Meyerhofer, Phys. Rev. Lett. **78**, 626 (1997).
[15] J. S. Cohen, Phys. Rev. A **64**, 043412 (2001).
[16] R. Taïeb, V. Véniard, and A. Maquet, Phys. Rev. Lett. **87**, 053002 (2001).
[17] P. H. Bucksbaum, M. Bashkansky, and T. J. McIlrath, Phys. Rev. Lett. **58**, 349 (1987).
[18] Y.-H. Chuang *et al.*, J. Opt. Soc. Am. B **8**, 1226 (1991).
[19] J. Peatross, B. Buerke, and D. D. Meyerhofer, Phys. Rev. A **47**, 1517 (1993).
[20] Co-Netic AA alloy is manufactured by Magnetic Shield Corporation, Bensenville, IL 60106, USA.
[21] B. E. Sauer *et al.*, Phys. Rev. Lett. **68**, 468 (1992).
[22] M. V. Ammosov, N. B. Delone, and V. P. Krainov, Sov. Phys. JETP **64**, 1191 (1986).
[23] J. L. Krause, K. J. Schafer, and K. C. Kulander, Phys. Rev. Lett. **68**, 3535 (1992).
[24] M. J. Nandor *et al.*, Phys. Rev. A **60**, R1771 (1999).
[25] A. Scrinzi, M. Geissler, and T. Brabec, Phys. Rev. Lett. **83**, 706 (1999).
[26] S. I. Themelis, T. Mercouris, and C. A. Nicolaides, Phys. Rev. A **61**, 024101 (1999).